

Optical refrigeration

The idea of cooling a solid-state optical material by simply shining a laser beam onto it may seem counterintuitive, but this is rapidly becoming a promising technology for future cryocoolers. Here, we chart the evolution of the science of optical refrigeration in rare-earth-doped solids and semiconductors from its origins through to the present day.

MANSOOR SHEIK-BAHAE^{1*} AND RICHARD I. EPSTEIN^{1,2}

¹Optical Science and Engineering, Department of Physics & Astronomy, University of New Mexico, Albuquerque, New Mexico 87131, USA

²Los Alamos National Laboratory, Los Alamos, New Mexico 87545, USA

*e-mail: msb@unm.edu

The term ‘laser cooling’ is most often associated with cooling dilute gases of atoms or ions to extremely low temperatures by reducing their thermal translational energy. This area of science has progressed immensely, resulting in physics Nobel prizes in 1997 and 2001 (refs 1,2). However, what many people don’t realize is that 46 years before such Doppler cooling of atoms was ever contemplated³, German physicist Peter Pringsheim suggested the possibility of cooling solids by means of fluorescence up-conversion⁴. In the solid phase, atoms do not have relative translational motion — their thermal energy is largely contained in the vibrational modes of the lattice. Laser cooling of solids (or optical refrigeration) is similar to atom cooling: light quanta in the red tail of the absorption spectrum are absorbed from a monochromatic source followed by spontaneous emission of more energetic (blue-shifted) photons. In the case of solids, the extra energy is extracted from lattice phonons, the quanta of vibrational energy in which heat is contained. The removal of these phonons cools the solid.

Laser cooling of solids can be exploited to achieve an all-solid-state cryocooler^{5,6}. The advantages of compactness, the absence of vibrations and moving parts or fluids, high reliability and the ability to operate without cryogenics have motivated intensive research. Space-borne infrared sensors will probably be the first beneficiaries, with other applications that require compact cryocooling reaping the benefits as the technology progresses. A study by Ball Aerospace⁷ shows that in low-power, space-borne operations, ytterbium-based optical refrigeration could outperform conventional thermoelectric and mechanical coolers in the temperature range between 80–170 K.

The process of optical refrigeration can occur only in special high-purity materials that have appropriately spaced energy levels and emit light with high quantum efficiency. So far, optical refrigeration research has been confined to either glasses and crystals doped with rare-earth (RE) elements or direct-bandgap semiconductors such as gallium arsenide. Although laser cooling of RE-doped solids has been successfully demonstrated, observation of net cooling in semiconductors, has so far remained elusive. Figure 1 schematically depicts the optical refrigeration

processes for a two-level system with broad ground- and excited-state manifolds. Photons from a low-entropy light source (that is, a laser) with energy, $h\nu$, excite atoms from the top of the ground state to the bottom of the excited state. The excited atoms reach quasi-equilibrium with the lattice by absorbing phonons. Spontaneous emission (fluorescence) follows with a mean photon energy, $h\nu_f$, that is higher than that of the absorbed photon. This process has also been called anti-Stokes fluorescence. There were concerns that the second law of thermodynamics might be violated until Landau clarified the issue in 1946 by assigning an entropy to the radiation⁸.

In the above picture, the interaction rate between electrons and phonons within each manifold is assumed to be far faster than the spontaneous-emission rate, which is valid for a broad range of materials and temperatures. The cooling efficiency or fractional cooling energy for each photon absorbed is

$$\eta_c = \frac{h\nu_f - h\nu}{h\nu} = \frac{\lambda}{\lambda_f} - 1, \quad (1)$$

where $\lambda = c/\nu$ is the wavelength of the laser and λ_f is the mean wavelength of spontaneous emission. The invention of the laser prompted several unsuccessful attempts to observe the effect experimentally^{9–11}. In 1995, net laser cooling in solids was first achieved by workers at Los Alamos National Laboratory¹² (LANL). Two technical challenges were addressed and overcome in these experiments. The LANL researchers had to have a system in which the vast majority of optical excitations recombine radiatively and where there is a minimal amount of parasitic heating due to unwanted impurities. Both of these critical engineering issues are ignored in the idealized situation described by equation (1), but are key to experimental success.

It is also important that spontaneously emitted photons escape the material without being trapped and re-absorbed, which would effectively inhibit spontaneous emission^{13,14}. This is a critical issue for high-refractive-index semiconductors, where total internal reflection can cause strong radiation trapping. In the absence of radiation trapping, the fraction of atoms that decay to the ground state by the desired radiative process is known as the quantum efficiency, $\eta_q = W_{\text{rad}}/(W_{\text{rad}} + W_{\text{nr}})$, where W_{rad} and W_{nr} are radiative and non-radiative decay rates, respectively. An external quantum efficiency, which includes a fluorescence escape efficiency, η_e , is defined by $\eta_{\text{ext}} = \eta_e W_{\text{rad}}/(\eta_e W_{\text{rad}} + W_{\text{nr}})$. This describes the efficiency by which a photo-excited atom decays into an escaped fluorescence photon. In a similar fashion, an absorption efficiency, $\eta_{\text{abs}} = \alpha_r/(\alpha_r + \alpha_b)$, is defined to account for the fraction of pump-laser photons that are engaged in cooling¹⁵. Here α_r is the

Report Documentation Page

Form Approved
OMB No. 0704-0188

Public reporting burden for the collection of information is estimated to average 1 hour per response, including the time for reviewing instructions, searching existing data sources, gathering and maintaining the data needed, and completing and reviewing the collection of information. Send comments regarding this burden estimate or any other aspect of this collection of information, including suggestions for reducing this burden, to Washington Headquarters Services, Directorate for Information Operations and Reports, 1215 Jefferson Davis Highway, Suite 1204, Arlington VA 22202-4302. Respondents should be aware that notwithstanding any other provision of law, no person shall be subject to a penalty for failing to comply with a collection of information if it does not display a currently valid OMB control number.

1. REPORT DATE DEC 2007		2. REPORT TYPE		3. DATES COVERED 00-00-2007 to 00-00-2000	
4. TITLE AND SUBTITLE Optical refrigeration				5a. CONTRACT NUMBER	
				5b. GRANT NUMBER	
				5c. PROGRAM ELEMENT NUMBER	
6. AUTHOR(S)				5d. PROJECT NUMBER	
				5e. TASK NUMBER	
				5f. WORK UNIT NUMBER	
7. PERFORMING ORGANIZATION NAME(S) AND ADDRESS(ES) University of New Mexico, Department of Physics & Astronomy, Albuquerque, NM, 87131				8. PERFORMING ORGANIZATION REPORT NUMBER	
9. SPONSORING/MONITORING AGENCY NAME(S) AND ADDRESS(ES)				10. SPONSOR/MONITOR'S ACRONYM(S)	
				11. SPONSOR/MONITOR'S REPORT NUMBER(S)	
12. DISTRIBUTION/AVAILABILITY STATEMENT Approved for public release; distribution unlimited					
13. SUPPLEMENTARY NOTES					
14. ABSTRACT					
15. SUBJECT TERMS					
16. SECURITY CLASSIFICATION OF:			17. LIMITATION OF ABSTRACT	18. NUMBER OF PAGES	19a. NAME OF RESPONSIBLE PERSON
a. REPORT unclassified	b. ABSTRACT unclassified	c. THIS PAGE unclassified			

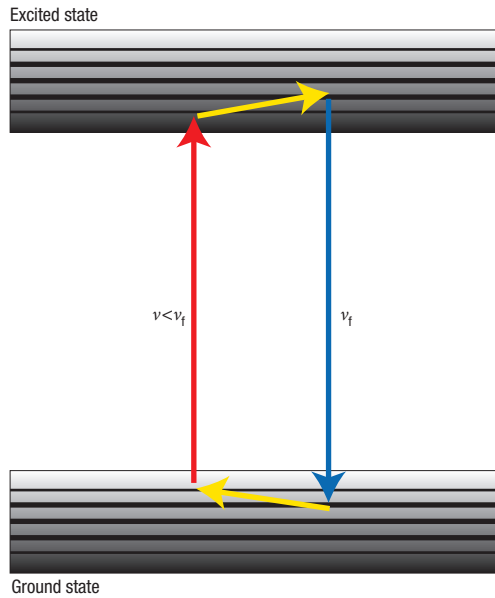


Figure 1 An energy diagram showing one way anti-Stokes fluorescence could occur. An atom with two broad levels is embedded in an otherwise transparent solid. The light source of frequency $h\nu$ (red arrow) excites atoms near the top of the ground-state level to the bottom of the excited state. Radiative decays, following interaction between the electrons and phonons (yellow arrows), emit photons with average energy $h\nu_f > h\nu$ (blue arrow).

resonant absorption coefficient and α_b is the unwanted parasitic (background) absorption coefficient. The combination of all these effects defines the cooling efficiency, $\eta_c = \eta_{\text{ext}}\eta_{\text{abs}}(\lambda/\lambda_f) - 1$, where the product $\eta_{\text{ext}}\eta_{\text{abs}}$ indicates the efficiency of converting an absorbed laser photon to an escaped fluorescence photon. Note that η_{abs} is frequency-dependent and falls off rapidly below photon energy $h\nu_f - k_B T$ where k_B is Boltzmann's constant and T is the lattice temperature. At very low pump-photon energy, η_{abs} will decrease enough to make $\eta_c < 0$ and laser cooling unattainable. The above analysis defines the condition needed for laser cooling¹⁵:

$$\eta_{\text{ext}}\eta_{\text{abs}} > 1 - \frac{k_B T}{h\nu} \tag{2}$$

This relation quantifies the needed efficiencies: cooling a material from room temperature with a nominal energy gap (pump photon) of 1 eV from room temperature demands that $\eta_{\text{ext}}\eta_{\text{abs}} > 97\%$. Although suitable lasers were available in the early 1960s, more than three decades of progress in material growth were needed to satisfy this condition.

COOLING RARE-EARTH-DOPED SOLIDS

The advantages of RE-doped solids for laser cooling have been foreseen for decades. Kastler and Yatsiv suggested these materials could be used for optical cooling as long ago as 1950 (ref. 9) and 1961 (ref. 11), respectively. The key optical transitions in RE-doped ions involve 4f electrons that are shielded by the filled 5s and 5p outer shells, which limit interactions with the surrounding lattice. Non-radiative decay due to multi-phonon emission is thus suppressed. Hosts with low phonon energy (such as fluoride crystals

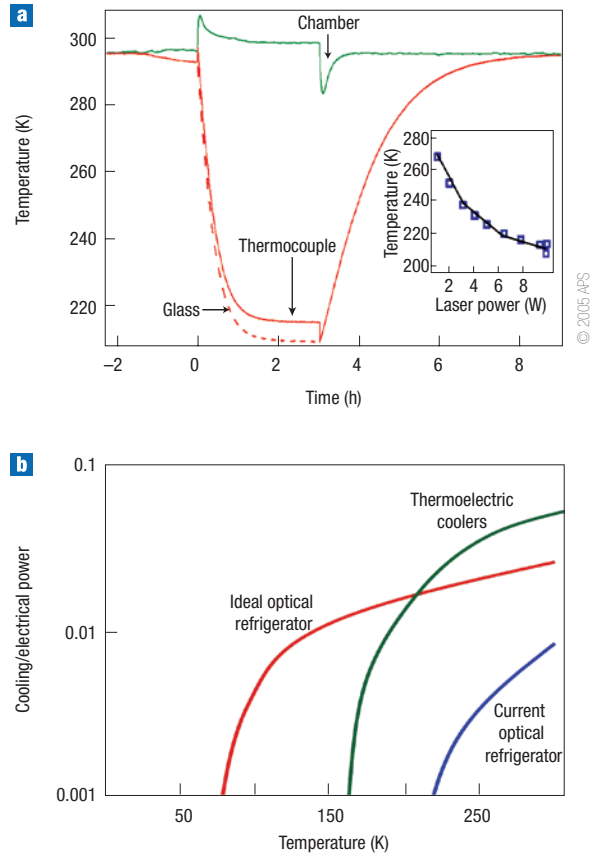


Figure 2 Optical cooling performance. **a**, The record cooling to 208 K with ZBLANP:Yb³⁺. The temperatures of the glass and the chamber were measured with thermocouples, from which the internal temperature of the glass was inferred. The inset shows the minimum glass temperature obtained as a function of pump laser. Reprinted with permission from ref. 19. **b**, A comparison of the cooling efficiencies of available thermoelectric coolers with ZBLANP:Yb³⁺-based optical refrigerators. Devices based on materials with low parasitic heating outperform thermoelectric coolers below 200 K, but optical coolers using current materials are less efficient than thermoelectric coolers at all temperatures³⁴. Data from refs 34,55.

and glasses) further diminish non-radiative decay and hence boost quantum efficiency. In 1968, Kushida and Geusic¹⁰ attempted to cool a Nd³⁺:YAG crystal with 1,064-nm laser radiation. They reported a reduction of heating, but no cooling; it is unclear whether they observed any anti-Stokes cooling effects. Laser cooling of a solid was first demonstrated experimentally in 1995 with the ytterbium-doped fluorozirconate glass ZBLANP:Yb³⁺ (ref. 12). Laser-induced cooling has since been observed in a range of glasses and crystals doped with Yb³⁺ (ZBLANP (refs 16–19), ZBLAN (refs 20,21), CNBZn (refs 22,23), BIG (refs 23,24), KGd(WO₄)₂ (ref. 22), KY(WO₄)₂ (ref. 22), YAG (ref. 25), Y₂SiO₅ (ref. 25), KPb₂Cl₅ (refs 23,26) and BaY₂F₈ (refs 27,28)).

In 2000, laser cooling in Tm³⁺-doped ZBLANP was reported at $\lambda \approx 1.9 \mu\text{m}$ (ref. 29). The significance of this result was twofold. First, it verified the scaling law of equation (1) by demonstrating an enhancement of nearly a factor of two in the cooling efficiency (compared with Yb-doped systems) to a value in agreement with the ratio of the corresponding cooling transition wavelengths. Second, it was the first demonstration of laser cooling in the presence of excited-state absorption. A record cooling power of approximately

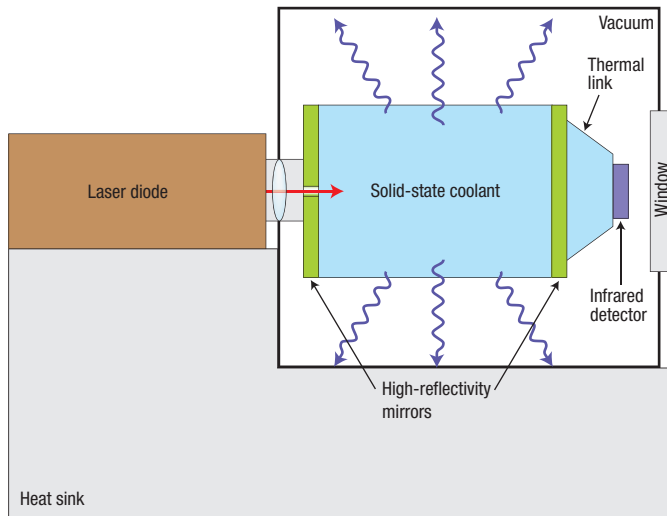


Figure 3 Schematic of an optical refrigeration system. Pump light is efficiently generated by a semiconductor laser diode and carried to the mirrored cooler element by an optical fibre. The laser enters the cooler through a pinhole in one mirror and is trapped by the mirrors until it is absorbed. Isotropic fluorescence escapes the cooler element and is absorbed by the coated vacuum casing. The load to be cooled, for example an infrared detector, is connected in the shadow region of the second mirror.

73 mW was later reported in this material by using a multipass geometry³⁰. More recently, cooling of Er³⁺-doped glass (CNBZn) and crystal (KPb₂Cl₂) has been reported at $\lambda \approx 0.870 \mu\text{m}$ (ref. 31). It is interesting to note that the cooling transition used in these experiments is between the ground state and the fourth excited state (⁴I_{9/2}) of Er³⁺, and not the first excited state as illustrated in Fig. 1. Although such high-energy transitions have a lower cooling efficiency (equation 1), they offer an effectively higher quantum efficiency owing to their low non-radiative decay rates to the ground state. Furthermore, as in the case of Tm³⁺ (ref. 29), the presence of higher excited states in Er³⁺ may prove advantageous because the energy transfer up-conversion transitions are endothermic (at the cooling wavelengths of the main transition) and have a high quantum efficiency^{31,32}.

The initial proof-of-principle experiments in ZBLANP:Yb³⁺ achieved only 0.3 K below ambient temperature¹². More recently, the LANL group has cooled ZBLANP:Yb³⁺ from room temperature to 208 K (ref. 19). Although progress is being made, optical refrigerators need to be more efficient and operate at lower temperatures to be competitive with other solid-state coolers, such as thermoelectric (Peltier) devices (see Fig. 2). Several studies^{5,25,33,34} have shown that ytterbium- or thulium-doped solids can potentially provide efficient cooling at temperatures well below 100 K.

There are several factors that limit the cooling of RE-doped solids both in theory and in practice owing to the nature of realizable materials. The most significant factor is the choice of laser-cooling medium. The ideal cooling efficiency (equation (1)) shows that there is an advantage if an optical refrigerator is pumped with lower-energy photons. This fact was part of the motivation for investigating thulium-doped cooling materials, because their ground- and excited-state manifolds are separated by about 0.6 eV, compared with 1.2 eV in ytterbium-doped solids. Weighing against this advantage are two other considerations. First is the choice of the pump laser, with fewer sources readily available near 0.6 eV. Although not a fundamental consideration,

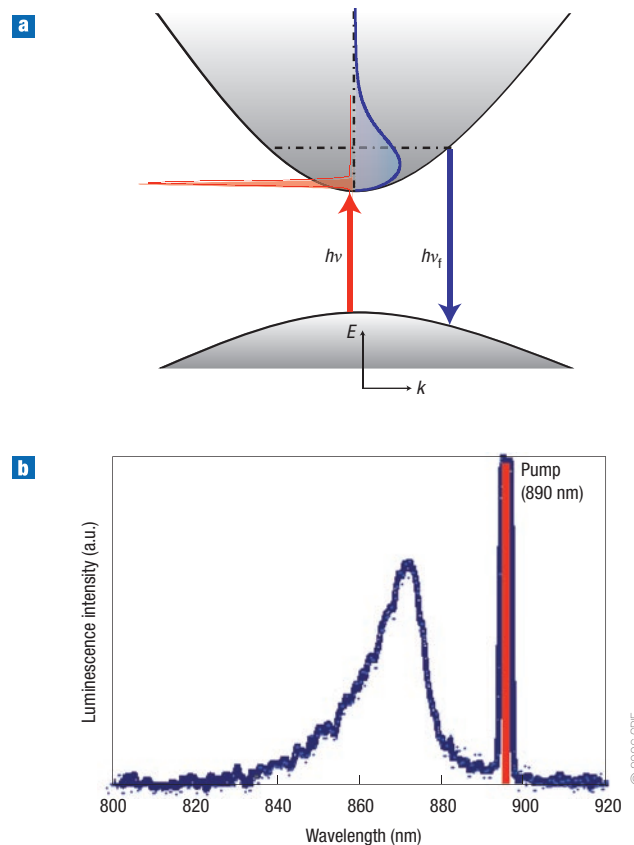


Figure 4 Semiconductor optical cooling. **a**, Cooling cycle in laser refrigeration of a semiconductor in which absorption of laser photons with energy $h\nu$ (shown in red) creates a cold distribution of electron-hole carriers (shown in blue, where E is energy and k is wave vector). Only the electron distribution is shown for clarity. The carriers then heat up through absorbing phonons, which is followed by an up-converted luminescence at $h\nu_1$. **b**, A typical anti-Stokes luminescence observed in GaAs/GaN double heterostructure. Reprinted with permission from ref. 15.

it needs to be kept in mind for commercialization plans that can be realized in the near future. A second and more general reason lies in the ratio of radiative to non-radiative relaxation decays. The rate of non-radiative, heat-producing, multi-phonon decay decreases exponentially with the separation between the two manifolds; this is the well-known energy-gap law. In practical terms, this means that because of the relatively large energy of the excited level in ytterbium-doped materials, non-radiative decays do not significantly decrease the quantum efficiency. However, for a pure thulium-doped material, non-radiative decays can overwhelm the anti-Stokes cooling, depending on the properties of the host material. For materials with low maximum phonon energies, such as ZBLANP (and other fluoride hosts), the non-radiative decays are relatively slow, whereas for many thulium-doped oxide crystals and glasses rapid non-radiative decays prevent laser cooling.

Another consideration in the choice of cooling medium is the width of the ground-state manifold. According to the Boltzmann distribution, the lower energy levels in the manifold are more populated than the higher ones. As the temperature falls and $k_B T$ becomes small compared with the energy width of the ground-state manifold, the upper levels become depopulated, leading to a decrease in the material opacity at lower frequencies. The net effect is that at low temperatures the cooling material

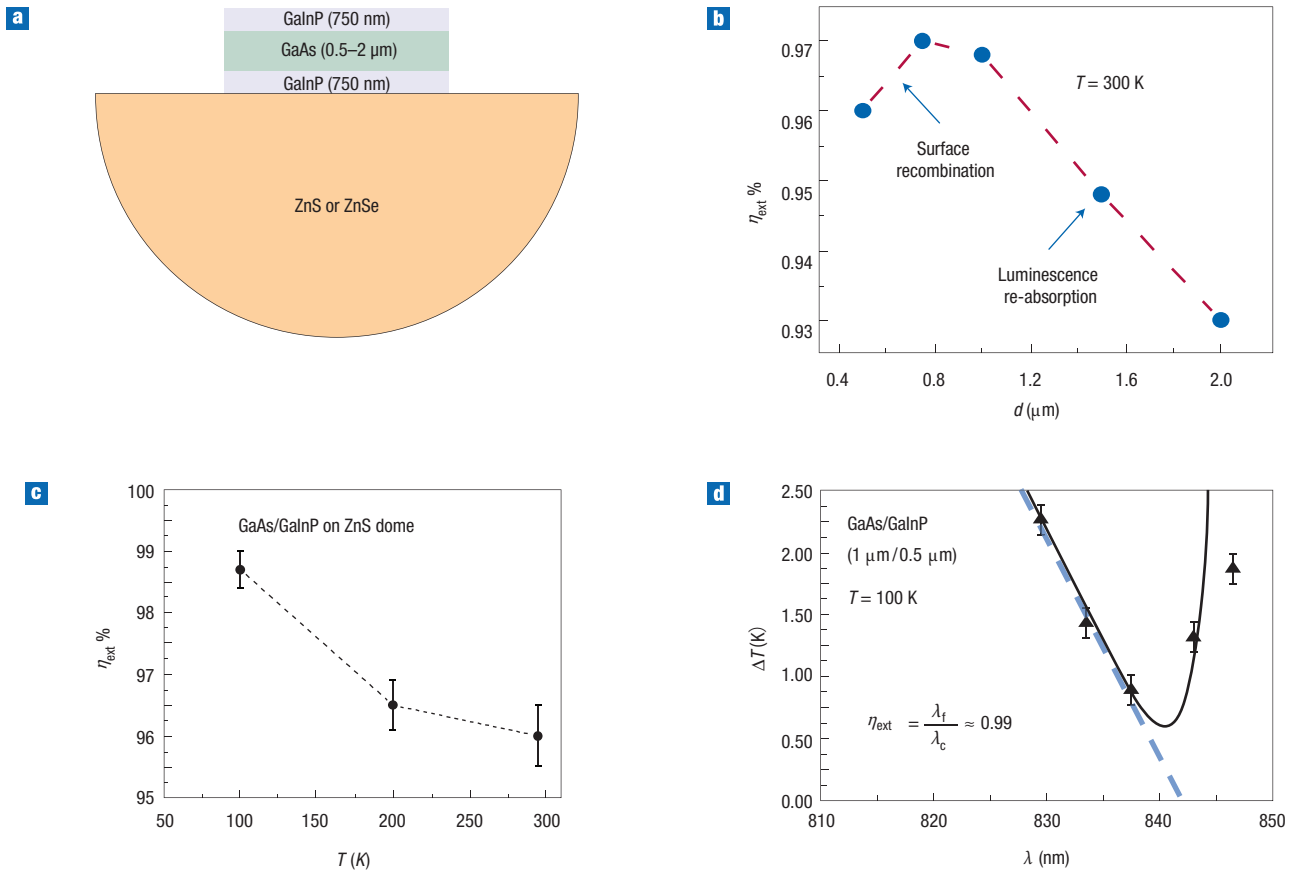


Figure 5 The external quantum efficiency. **a**, The GaAs/GaNp double heterostructure is bonded to a nearly index-matched dome (ZnS or ZnSe) to enhance its luminescence extraction. **b**, External quantum efficiency measured at room temperature in a bonded sample of the heterostructure in **a** for various GaAs thicknesses (d), with the GaNp layer thickness fixed at 750 nm. **c**, Measured η_{ext} versus lattice temperature for a GaAs thickness of 1 μm . **d**, Fractional heating of 1- μm -thick GaAs sample as a function of excitation wavelength for a fixed (optimum) electron–hole density at a starting temperature of 100 K. The extrapolation of short-wavelength data determines the zero-crossing wavelength from which a record η_{ext} of about 99% is deduced. Excitation at longer wavelengths causes heating due to background parasitic absorption^{15,51} as indicated by the solid line calculated assuming $\alpha_0 = 10 \text{ cm}^{-1}$. **b,c,d** Reprinted with permission from ref. 15, copyright (2006) SPIE, and ref. 51.

cannot be pumped at frequencies below ν_p and cooling becomes impossible, see equation (1). The width of the ground-state manifold is a result of crystal field splitting and depends on both the dopant ion and the host material. By choosing ions and a host that give narrow ground-state manifolds, the material can cool to lower temperatures before the low-frequency transparency condition sets in.

For the material systems studied so far, the limitation on achieved cooling is not due to the reasons outlined above, but is more likely to be the result of parasitic heating from unwanted impurities in the bulk of the cooling material or on its surface. As can be seen in Fig. 2b, the cooling efficiencies of ZBLANP:Yb³⁺ available at present are far below that for an ideal material with no parasitic heating. One important source of heating in this material is quenching of excited ytterbium ions by impurities, such as iron and copper. The radiative decay time of an excited Yb³⁺ ion is about 1 ms. During this time, the excitation migrates through the glass by transferring energy to neighbouring ions. If the excitation encounters an impurity atom, the energy can be transferred to this atom and be rapidly converted into heat. A detailed study by Hehlen and co-workers³⁴ found that close to ideal cooling efficiency could be achieved when the concentration of impurities is 0.01 p.p.m. for Cu²⁺ and 0.1 p.p.m. for Fe²⁺.

An additional source of parasitic heating is absorption in the mirrors that trap the pump radiation in the cooling element. In the LANL experiments the cooling glass has a pair of high-reflectivity mirrors deposited on two surfaces, as indicated in Fig. 3. Pump light is reflected many times by each mirror, so that even relatively low absorption of 0.0001 per reflection produces significant heating. Depositing a higher-quality dielectric mirror may obviate this problem. An alternative approach is to use an optical-cavity configuration to enhance the pump absorption. Both intra-laser-cavity²¹ and external-resonant-cavity³⁵ geometries have been demonstrated. The external-resonant-cavity approach used at the University of New Mexico has been shown to be capable of achieving pump absorption exceeding 90% (ref. 35). It has also been proposed that photon localization in nanocrystalline powders can be exploited to enhance laser-pump absorption in the cooling of RE-doped systems³⁶.

WILL SEMICONDUCTORS COOL?

In addition to the studies of optical refrigeration in RE-doped materials, researchers have examined other condensed-matter systems including semiconductors^{37–40}. Semiconductor coolers provide more efficient pump-light absorption, the potential for

much lower temperatures, and the opportunity for direct integration into electronics and photonics. These materials provide their own set of engineering challenges, however, and no net cooling has been observed yet. The essential difference between semiconductors and RE-doped materials is in their cooling cycles. In RE-doped materials, the cooling transition occurs in localized donor ions within the host material, whereas the cooling cycles in semiconductors involves transitions between extended valence and conduction bands of a direct-bandgap semiconductor (see Fig. 4a). Indistinguishable charge carriers in the Fermi–Dirac distribution may enable semiconductors to become much colder than RE materials. The highest energy levels of the ground-state manifold in the RE-doped systems become less populated as the temperature is lowered, owing to Boltzmann statistics. As discussed in the previous section, the cooling cycle will ultimately cease as the lattice temperature becomes comparable to the width of the ground state. This corresponds to $T \approx 100$ K for most existing RE-doped systems. No such limitation exists in pure (undoped) semiconductors — temperatures as low as 10 K may be achievable^{13,15,41}.

Semiconductors should achieve a higher cooling power density (rate of heat removal) compared with RE-materials. The maximum cooling power density is about $Nk_b T/\tau_r$, where N is the photo-excited-electron (-hole) density and τ_r is the radiative recombination time. The excitation density does not provide an advantage; in fact, optimal N is limited owing to many-body processes, and does not exceed that of moderately doped RE systems. However, we can gain five to six orders of magnitude in cooling power density as the radiative recombination rates in semiconductors are much faster than in RE ions.

There have been a number of theoretical investigations^{13,38,41–43} as well as a few experimental attempts to achieve laser cooling with semiconductors^{40,44–46}. A feasibility study by the authors of this review outlined the conditions for net cooling based on fundamental material properties and light management¹³. Researchers at the University of Arizona⁴¹ studied luminescence up-conversion in the presence of partially ionized excitons, and developed a microscopic theory for laser cooling that provides valuable predictive capabilities for low-temperature operations. The possible enhancements of laser cooling by including the effects of the photon density of states as well as luminescence coupling schemes based on surface plasmon polaritons were recently introduced by J. B. Khurgin at Johns Hopkins University^{47,48}. The first thorough experimental effort was reported by the University of Colorado⁴⁴. No net cooling was achieved, despite realization of an impressive external quantum efficiency of 96% in GaAs. These experiments used a high-quality heterostructure in optical contact with a ZnSe dome structure for enhanced luminescence extraction. A report of local cooling in AlGaAs quantum wells by a European consortium⁴⁴ was later attributed to misinterpretation of spectra caused by Coulomb screening of the excitons⁴⁹.

Figure 4b shows anti-Stokes luminescence in a GaAs heterostructure, where excitation at $\lambda = 890$ nm produces broadband luminescence with a mean wavelength of $\lambda_f \approx 860$ nm. Each luminescent photon carries away about 40 meV more energy than an absorbed photon adds, so cooling might be expected. Why then have we not been able to observe laser cooling in this material or any semiconductor? To answer this question we have to go back to the cooling condition of equation (2), where η_{ext} is modified to include the presence of many-body interactions, yielding an expression dependent on N :

$$\eta_{\text{ext}} = \frac{\eta_c B N^2}{A N + \eta_c B N^2 + C N^3}, \quad (3)$$

where A , B and C are decay coefficients. The radiative recombination rate $B N^2$ indicates the bimolecular nature of electron–hole

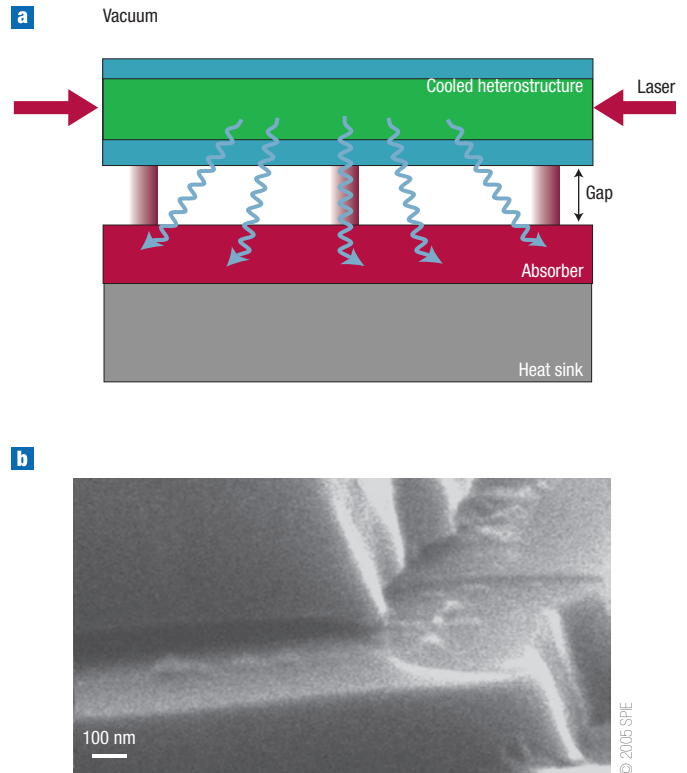


Figure 6 A vacuum ‘nanogap’ structure where the heterostructure is situated (for example, supported by posts) at a subwavelength distance from an absorber. **a**, Schematic of the structure. Luminescence photons will escape into the absorber by frustrated total internal reflection (photon tunnelling) and the gap provides a thermal barrier. **b**, Scanning electron micrograph of a preliminary nanogap structure (with 50-nm spacing) fabricated using a multi-step photolithographic technique. Reprinted with permission from ref. 52.

recombination (again, a consequence of ‘indistinguishability’). The non-radiative recombination rate is determined by A and is dominated by the surface recombination in a high-purity semiconductor⁴⁶. At high N , luminescence efficiency degrades owing to the three-body Auger recombination, determined by the coefficient C . It follows from equation (3) that there is an optimal carrier density that maximizes the external quantum efficiency, a condition not present in RE-materials. A further complication is the poor luminescence escape efficiency (η_c) in high-index semiconductors, such as GaAs. Total internal reflection causes the majority of the spontaneous emission to get trapped and re-absorbed. A similar problem limits the efficiency of LEDs. For a bulk pure semiconductor, the coefficients B and C are fixed, fundamental properties. Researchers can manipulate η_c and A by fabrication and growth procedures to satisfy the cooling condition. Highly controlled epitaxial growth techniques, such as metal–organic chemical vapour deposition (MOCVD) can produce very low surface recombination rates ($A < 1.5 \times 10^4 \text{ s}^{-1}$). This involves a double heterostructure of GaAs/GaInP as shown in Fig. 5a, where the lattice-matched cladding layers provide surface passivation as well as carrier confinement. To deal with extraction efficiency, geometric coupling schemes (such as nearly index-matched dome lenses, as shown also in Fig. 5a) have been used to enhance η_c to 15–20%. This has resulted in a measured η_{ext} of 97% at room temperature, which is not quite sufficient for net cooling^{40,46,50,51}. The optimum GaAs thickness is found to be

about 1 μm , determined by excessive luminescence re-absorption for thicker layers and surface recombination for thinner layers⁴⁶, as shown in Fig. 5b. Improvements in luminescence extraction as well as surface passivation are needed to cool semiconductors from room temperature.

The temperature dependence of η_{ext} is an important factor. It is fortuitous that B increases while A and C decrease as the temperature drops. Low temperatures thus shift the external quantum efficiency closer to unity, according to equation (3). A record efficiency of 99% has been observed in a GaAs/GaInP double heterostructure at $T = 100\text{ K}$ (Fig. 5c,d and ref. 51). The experiment involved measuring the temperature of the heterostructure that was van der Waals bonded to a ZnS dome as the Ti:sapphire pump laser was tuned around the mean luminescence wavelength. The excitation density was kept constant by monitoring the total luminescence as the laser wavelength was varied. The temperature change induced by the pump laser is directly proportional to the cooling efficiency^{15,40,51}. In the short-wavelength regime, the absorption efficiency can be considered to be unity, and the data follows a line represented by $1 - \eta_{\text{ext}}\lambda/\lambda_r$. The extrapolation of this line crosses the x axis at the (zero) crossing wavelength λ_c , for which $1 - \eta_{\text{ext}}\lambda_c/\lambda_r = 0$. This gives a rather precise measurement of η_{ext} . The record 99% efficiency from this measurement is sufficiently high for net cooling^{15,51}. The presence of the parasitic absorption, however, hinders this process as the sample heats at longer ($\lambda > \lambda_r$) wavelengths. An initial parametric study points to the GaAs layer itself as the possible source of parasitic absorption. Various efforts are under way to address this material problem by researchers at the National Renewable Energy Laboratory and the University of New Mexico. In addition to highly controlled MOCVD growth, aluminium-free GaAs heterostructure growth using phosphorous molecular-beam epitaxy is now being explored to obtain cooling-grade materials.

Although it is essential to improve the absorption efficiency by lowering the parasitic background absorption, methods to enhance η_{ext} by improving luminescence extraction efficiency are being explored as well. A method based on the frustrated total internal reflection across a vacuum ‘nanogap’ is being developed at the University of New Mexico^{15,52,53}. In this scheme, the luminescence photons tunnel through the gap into the absorber region with the vacuum nanogap maintaining a thermal barrier between the heterostructure and the absorber or heat sink. Calculations show that a gap spacing of less than 25 nm outperforms the dome structure (GaAs on ZnS or ZnSe), and preliminary fabrication of such structures show promising results. Using a multi-step photolithographic process, a silicon-based nanogap with 50-nm spacing supported by posts (with sufficiently low fill factor) has been monolithically fabricated as depicted in Fig. 6 (ref. 52). Recently, we have fabricated GaAs nanogap structures that will be integrated with a high-quality GaAs heterostructure to investigate their performance in cooling experiments.

FUTURE OUTLOOK

Optical refrigeration has advanced from basic principles to a promising technology. Cooling of RE-based materials is fast approaching cryogenic operation. In semiconductors, much progress has been made in achieving a high η_{ext} . With the advanced heterostructure growth and novel device fabrication underway at present, cooling will soon be attainable. In the next few years, optical refrigeration should be useful in applications such as satellite instrumentation, where compactness, ruggedness and the lack of vibrations are important. Many more applications would be possible if the basic efficiency of optical refrigerators of about $k_B T/h\nu$ can be improved. This efficiency limit assumes all fluorescence photons are

absorbed by a heat sink and thus wasted. If these photons can be recycled by means of photovoltaic devices, then the efficiency can be improved⁵⁴. If the efficiency of photovoltaic cells and pump laser diodes approach their thermal limit of about $1 - k_B T_R/E_g$, where T_R is the ambient or reservoir temperature and E_g is the bandgap energy, then the overall efficiency will approach the Carnot limit. Optical refrigerators clearly have the potential to make a significant impact on electronics and photonics in the future.

doi:10.1038/nphoton.2007.244

References

1. Chu, S., Cohen-Tannoudji, C. & Philips, W. D. For development of methods to cool and trap atoms with laser light. *Nobel Prize in Physics* (1997); <http://nobelprize.org>.
2. Cornell, E. A., Ketterle, W. & Weiman, C. E. For the achievement of Bose-Einstein condensation in dilute gases of alkali atoms, and for early fundamental studies of the properties of the condensates. *Nobel Prize in Physics* (2001); <http://nobelprize.org>.
3. Hänsch, T. W. & Schawlow, A. L. *Opt. Commun.* Cooling of gases with laser radiation. **13**, 68–69 (1975).
4. Pringsheim, P. Zwei bemerkungen über den Unterschied von lumineszenz- und temperaturstrahlung. *Z. Phys.* **57**, 739–746 (1929).
5. Edwards, B. C., Buchwald, M. I. & Epstein, R. I. Development of the Los-Alamos solid-state optical refrigerator. *Rev. Sci. Instrum.* **69**, 2050–2055 (1998).
6. Edwards, B. C., Anderson, J. E., Epstein, R. I., Mills, G. L. & Mord, A. J. Demonstration of a solid-state optical cooler: An approach to cryogenic refrigeration. *J. Appl. Phys.* **86**, 6489–6493 (1999).
7. Mills, G. & Mord, A. Performance modeling of optical refrigerators. *Cryogenics* **46**, 176–182 (2005).
8. Landau, L. On the thermodynamics of photoluminescence. *J. Phys. (Moscow)* **10**, 503–506 (1946).
9. Kastler, A. Some suggestions concerning the production and detection by optical means of inequalities in populations of levels of spatial quantization in atoms. *J. Phys. Radium* **11**, 255–265 (1950).
10. Kushida, T. & Geusic, J. E. Optical refrigeration in Nd-doped yttrium aluminum garnet. *Phys. Rev. Lett.* **21**, 1172–1175 (1968).
11. Yatsiv, S. in *Advances in Quantum Electronics* (ed. Singer, J. R.) 200–213 (Columbia Univ. Press, New York, 1961).
12. Epstein, R. I., Buchwald, M. I., Edwards, B. C., Gosnell, T. R. & Mungan, C. E. Observation of laser-induced fluorescent cooling of a solid. *Nature* **377**, 500–503 (1995).
13. Sheik-Bahae, M. & Epstein, R. I. Can laser light cool semiconductors? *Phys. Rev. Lett.* **92**, 247403 (2004).
14. Asbeck, P. Self-absorption effects on radiative lifetime in GaAs-GaAlAs double heterostructures. *J. Appl. Phys.* **48**, 820–822 (1977).
15. Sheik-Bahae, M., Imangholi, B., Hasselbeck, M. P., Epstein, R. I. & Kurtz, S. in *Proc. SPIE: Phys. Simulation Optoelectron. Devices XIV* (eds Osinski, M., Henneberger, F. & Arakawa, Y.) **6115**, 611518 (2006).
16. Mungan, C. E., Buchwald, M. I., Edwards, B. C., Epstein, R. I. & Gosnell, T. R. Laser cooling of a solid by 16 K starting from room-temperature. *Phys. Rev. Lett.* **78**, 1030–1033 (1997).
17. Luo, X., Eissaman, M. D. & Gosnell, T. R. Laser cooling of a solid by 21 K starting from room temperature. *Opt. Lett.* **23**, 639–641 (1998).
18. Gosnell, T. R. Laser cooling of a solid by 65 K starting from room temperature. *Opt. Lett.* **24**, 1041–1043 (1999).
19. Thiede, J., Distel, J., Greenfield, S. R. & Epstein, R. I. Cooling to 208 K by optical refrigeration. *Appl. Phys. Lett.* **86**, 154107 (2005).
20. Rayner, A. et al. Laser cooling of a solid from ambient temperature. *J. Mod. Opt.* **48**, 103–114 (2001).
21. Heeg, B. et al. Experimental demonstration of intracavity solid-state laser cooling of $\text{Yb}^{3+}:\text{ZrF}_2\text{-BaF}_2\text{-LaF}_3\text{-AlF}_3\text{-NaF}$ glass. *Phys. Rev. A* **70**, 021401 (2004).
22. Bowman, S. R. & Mungan, C. E. New materials for optical cooling. *Appl. Phys. B* **71**, 807–811 (2000).
23. Fernandez, J. R. et al. in *Proc. SPIE: Rare-Earth-Doped Mater. Dev. VI* (eds Jiang, S. & Keys, R. W.) **4645**, 135–147 (2002).
24. Fernandez, J., Mendioroz, A., García, A. J., Balda, R. & Adam, J. L. Anti-Stokes laser-induced internal cooling of Yb^{3+} -doped glasses. *Phys. Rev. B* **62**, 3213–3217 (2000).
25. Epstein, R. I., Brown, J. J., Edwards, B. C. & Gibbs, A. Measurements of optical refrigeration in ytterbium-doped crystals. *J. Appl. Phys.* **90**, 4815–4819 (2001).
26. Mendioroz, A. et al. Anti-stokes laser cooling in Yb^{3+} -doped KPb_2Cl_5 crystal. *Opt. Lett.* **27**, 1525–1527 (2002).
27. Bigotta, S. et al. Laser cooling of Yb^{3+} -doped BaY_2F_8 single crystal. *Opt. Mater.* **28**, 1321–1324 (2006).
28. Bigotta, S. et al. Spectroscopic and laser cooling results on Yb^{3+} -doped BaY_2F_8 single crystal. *J. Appl. Phys.* **100**, 013109 (2006).
29. Hoyt, C. W., Sheik-Bahae, M., Epstein, R. I., Edwards, B. C. & Anderson, J. E. Observation of anti-Stokes fluorescence cooling in thulium-doped glass. *Phys. Rev. Lett.* **85**, 3600–3603 (2000).
30. Hoyt, C. et al. Advances in laser cooling of thulium-doped glass. *J. Opt. Soc. Am. B* **20**, 1066–1074 (2003).
31. Fernandez, J., Garcia-Adeva, A. J. & Balda, R. Anti-Stokes laser cooling in bulk erbium-doped materials. *Phys. Rev. Lett.* **97**, 033001 (2006).
32. Garcia-Adeva, A. J., Balda, R. & Fernandez, J. in *Proc. SPIE: Laser Cooling Sol.* (eds Epstein, R. I. & Sheik-Bahae, M.) **6461**, 646102 (2007).
33. Lamouche, G., Lavallard, P., Suris, R. & Grousson, R. Low temperature laser cooling with a rare-earth doped glass. *J. Appl. Phys.* **84**, 509–516 (1998).
34. Hehlein, M. P., Epstein, R. I. & Inoue, H. Model of laser cooling in the Yb^{3+} -doped fluorozirconate glass ZBLAN. *Phys. Rev. B* **75**, 144302 (2007).
35. Seletskiy, D., Hasselbeck, M. P., Sheik-Bahae, M. & Epstein, R. I. in *Proc. SPIE: Laser Cooling Sol.* (eds Epstein, R. I. & Sheik-Bahae, M.) **6461**, 646103 (2007).
36. Ruan, X. L. & Kaviani, M. Enhanced laser cooling of rare-earth-ion-doped nanocrystalline powders. *Phys. Rev. B* **73**, 155422 (2006).

37. Clark, J. L. & Rumbles, G. Laser cooling in the condensed-phase by frequency up-conversion. *Phys. Rev. Lett.* **76**, 2037–2040 (1996).
38. Oraevsky, A. N. Cooling of semiconductors by laser radiation. *J. Russian Laser Res.* **17**, 471–479 (1996).
39. Rivlin, L. A. & Zadernovsky, A. A. Laser cooling of semiconductors. *Opt. Commun.* **139**, 219–222 (1997).
40. Gauck, H., Gfroerer, T. H., Renn, M. J., Cornell, E. A. & Bertness, K. A. External radiative quantum efficiency of 96% from a GaAs/GaN_P heterostructure. *Appl. Phys. A* **64**, 143–147 (1997).
41. Rupper, G., Kwong, N. H. & Binder, R. Large excitonic enhancement of optical refrigeration in semiconductors. *Phys. Rev. Lett.* **97**, 117401 (2006).
42. Huang, D. H., Apostolova, T., Alsing, P. M. & Cardimona, D. A. Spatially selective laser cooling of carriers in semiconductor quantum wells. *Phys. Rev. B* **72**, 195308 (2005).
43. Li, J. Z. Laser cooling of semiconductor quantum wells: Theoretical framework and strategy for deep optical refrigeration by luminescence upconversion. *Phys. Rev. B* **75**, 155315 (2007).
44. Finkeissen, E., Potemski, M., Wyder, P., Vina, L. & Weimann, G. Cooling of a semiconductor by luminescence up-conversion. *Appl. Phys. Lett.* **75**, 1258–1260 (1999).
45. Gfroerer, T. H., Cornell, E. A. & Wanlass, M. W. Efficient directional spontaneous emission from an InGaAs/InP heterostructure with an integral parabolic reflector. *J. Appl. Phys.* **84**, 5360–5362 (1998).
46. Imangholi, B., Hasselbeck, M. P., Sheik-Bahae, M., Epstein, R. I. & Kurtz, S. Effects of epitaxial lift-off on interface recombination and laser cooling in GaInP/GaAs heterostructures. *Appl. Phys. Lett.* **86**, 081104 (2005).
47. Khurgin, J. B. Surface plasmon-assisted laser cooling of solids. *Phys. Rev. Lett.* **98**, 177401 (2007).
48. Khurgin, J. B. Band gap engineering for laser cooling of semiconductors. *J. Appl. Phys.* **100**, 113116 (2006).
49. Hasselbeck, M. P., Sheik-Bahae, M. & Epstein, R. I. in *Proc. SPIE: Laser Cooling Sol.* (eds Epstein, R. I. & Sheik-Bahae, M.) **6461**, 646107 (2007).
50. Catchpole, K. R. *et al.* High external quantum efficiency of planar semiconductor structures. *Semiconductor Sci. Technol.* **19**, 1232–1235 (2004).
51. Imangholi, B. *Investigation of laser cooling in semiconductors*. Thesis, Univ. New Mexico (2006).
52. Martin, R. P. *et al.* in *Proc. SPIE: Laser Cooling Sol.* Vol. 6461 (eds Epstein, R. I. & Sheik-Bahae, M.) 6410H (SPIE, 2007).
53. Epstein, R. I., Edwards, B. C. & Sheik-Bahae, M. Semiconductor-based optical refrigerator. US Patent 6,378,321 (2002).
54. Edwards, B. C., Buchwald, M. I. & Epstein, R. I. Optical refrigerator using reflectivity tuned dielectric mirrors. US Patent 6,041,610 (2000).
55. Mills, G. L., Mord, A. J. & Slaymaker, P. A. Design and predicted performance of an optical cryocooler for a focal plane application. *Cryocoolers* **11**, 613–620 (2001).

Acknowledgements

This work has been supported by the Air Force Office of Scientific Research (MURI program), the National Aeronautics and Space Administration (NASA) and the US Department of Energy. The authors thank M. P. Hasselbeck and D. Seletskiy for reading the manuscript.